Plant Pathol. J. 35(5): 521-529 (2019)
https://doi.org/10.5423/PPJ.OA.04.2019.0120
pISSN 1598-2254 eISSN 2093-9280

The Plant Pathology Journal
©The Korean Society of Plant Pathology

Research Article **Open Access**

Tomato Yellow Leaf Curl China Virus Impairs Photosynthesis in the Infected *Nicotiana benthamiana* with βC1 as an Aggravating Factor

Tahir Farooq[1], Dandan Liu[1], Xueping Zhou[1,2], and Qiuying Yang[1,3]*

[1]*State Key Laboratory for Plant Disease and Insect Pest, Institute of Plant Protection, China Academy of Agricultural Sciences, Beijing 100193, China*
[2]*State Key Laboratory for Rice Biology, Institute of Biotechnology, Zhejiang University, Hangzhou 310058, China*
[3]*State Key Laboratory of Biocatalysis and Enzyme Engineering, College of Life Sciences, Hubei University, Wuhan 430062, China*

(Received on April 27, 2019; Revised on June 29, 2019; Accepted on July 18, 2019)

***Tomato yellow leaf curl China virus* is a species of the widespread geminiviruses. The infection of *Nicotiana benthamiana* by Tomato yellow leaf curl China virus (TYLCCNV) causes a reduction in photosynthetic activity, which is part of the viral symptoms. βC1 is a viral factor encoded by the betasatellite DNA (DNAβ) accompanying TYLCCNV. It is a major viral pathogenicity factor of TYLCCNV. To elucidate the effect of βC1 on plants' photosynthesis, we measured the relative chlorophyll (Chl) content and Chl fluorescence in TYLCCNV-infected and *βC1* transgenic *N. benthamiana* plants. The results showed that Chl content is reduced in TYLCCNV A–infected, TYLCCNV A plus DNAβ (TYLCCNV A + β)–infected and *βC1* transgenic plants. Further, changes in Chl fluorescence parameters, such as electron transport rate, F_v/F_m, *NPQ*, and *qP*, revealed that photosynthetic efficiency is compromised in the aforementioned *N. benthamiana* plants. The presense of *βC1* aggravated the decrease of Chl content and photosynthetic efficiency during viral infection. Additionally, the real-time quantitative PCR analysis of oxygen evolving complex genes in photosystem II, such as *PsbO*, *PsbP*, *PsbQ*, and *PsbR*, showed a significant reduction of the relative expression of these genes at the late stage of TYLCCNV A + β infection and at the vegetative stage of *βC1* transgenic *N. benthamiana* plants. In summary, this study revealed the pathogenicity of TYLCCNV in photosynthesis and disclosed the effect of βC1 in exacerbating the damage in photosynthesis efficiency by TYLCCNV infection.**

Keywords **:** βC1, betasatellite, Chl content, Chl fluorescence photosynthesis, Tomato yellow leaf curl China virus (TYLCCNV)

Handling Editor **:** Ju, Ho-Jong

In plant-virus interactions, chloroplast is a common target for viral pathogenesis/propagation, and photosynthesis-related factors play a key role in the development of disease symptoms (Zhao et al., 2016). The virus-induced disruption of chloroplasts' structure and function has been suggested to be connected with typical photosynthesis-related symptoms (Zhao et al., 2016).

Among plant viruses, *Begomovirus* is currently the largest genus with over 300 species identified (Brown et al., 2012). Begomoviruses are transmitted by whiteflies (*Bemisia tabaci*), and cause devastating diseases in fiber crops and vegetables worldwide (Brown et al., 2012; Inoue-Nagata et al., 2016). The typical symptoms that are caused by begomoviruses include mosaic, leaf curling, vein yellowing, general leaf yellowing, and stunted growth in the infected plants (Leke et al., 2015). Begomovirus-associated betasatellites are important in the induction of typical viral disease symptoms (Zhou, 2013). The coding sequences in betasatellites only encode a βC1 protein which, in addition to function as a suppressor of gene silencing, plays critical

*Corresponding author.
Phone) +86-27-88661571, FAX) +86-27-88661571
E-mail) qiuying.yang@hubu.edu.cn
This is an Open Access article distributed under the terms of the Creative Commons Attribution Non-Commercial License (http://creativecommons.org/licenses/by-nc/4.0) which permits unrestricted noncommercial use, distribution, and reproduction in any medium, provided the original work is properly cited.

Articles can be freely viewed online at www.ppjonline.org.

roles in symptoms development (Zhou, 2013). The βC1 of a begomovirus, Radish leaf curl virus (RaLCB), has been reported to contribute to photosynthesis-related viral symptoms through interfering with chloroplasts' ultrastructure and expression of photosystem genes (Bhattacharyya et al., 2015).

Tomato yellow leaf curl China virus (TYLCCNV) is a begomovirus which is known to infect tomato and tobacco, causing leaf curl symptom (Cui et al., 2004). The TYLCCNV-associated betasatellite encodes a βC1 which is known to be a major symptom determinant (Zhang et al., 2015; Zhou, 2013).

Previous studies described the effect of viral infection on plants' photosynthetic efficiency and expression of chloroplast proteins at the transcriptomic and proteomic levels, which shed light on the molecular events during symptom progression (Bhattacharyya et al., 2015). Following this clue, the present study aims to elucidate the putative roles of TYLCCNV and TYLCCNV betasatellite–encoded pathogenicity factor, βC1, in the development of photosynthesis-related disease symptoms. Our findings demonstrate that TYLCCNV A–, TYLCCNV A + β–infection and *βC1* transgene all reduced chlorophyll (Chl) content and affected Chl fluorescence transients in *Nicotiana benthamiana* plants. TYLCCNV A- and TYLCCNV A + β–infection triggered changes in Chl fluorescence transients even before the onset of symptoms, reflecting the inhibition of photosynthesis at the early stage of infection. Although the coinfection with betasatellite DNA (DNAβ) induced more severe impairment of photosynthesis efficiency and Chl reduction in TYLCCNV A + β– than in TYLCCNV A–infected plants, the reduction in transcription of oxygen evolving complex (OEC) genes occurred only at the late stage of TYLCCNV infection, suggesting that βC1 probably reduced the transcription of OEC genes through its accumulating virulent effect.

Materials and Methods

Plant materials and growth conditions. Wild type and *35S::βC1* transgenic (generated by Qiuying Yang according to the method described before) (Cui et al., 2004). *N. benthamiana* plants were grown in a substrate mixture containing artificial soil, vermiculite, perlite, and black soil (2:2:1:2), at 16 h-light/8 h-dark cycle with 150 µmol/m^2/s photosynthetically active radiation, a relative humidity of 60-65% and a temperature of 25-28ºC.

Agroinoculation of plants. *Agrobacterium tumefaciens* harboring TYLCCNV A and DNAβ (Y10 isolate) constructs were cloned by the previous lab members (Cui et al., 2004). These *Agrobacterium tumefaciens* clones were cultured separately in Luria-Bertani liquid medium at 28ºC until OD_{600} = 0.6, and then the bacteria were pelleted, resuspended in transformation buffer (10 mM $MgCl_2$, 100 mM MES, 100 µM acetosyringone, pH 5.7) to OD_{600} = 1and incubated in darkness for 2-3 h at room temperature. Afterwards, the transformation suspension containing TYLCCNV A and DNAβ were mixed in equal volume for co-inoculation, or TYLCCNV A suspension was used for inoculation alone. Mock inoculation was done by injecting only the transformation buffer. Wild type *N. benthamiana* leaves at the six leaf stage were injected with 0.2 ml of the suspension using a 1-ml needleless plastic syringe (Cui et al., 2004). After inoculation, plants were maintained in the above-mentioned growth conditions and regularly observed for the development of viral symptoms.

Measurement of Chl contents. The total Chl (Chl *a* + Chl *b*) contents of *N. benthamiana* leaves were measured *in situ* using a hand-held soil plant analysis development (SPAD)-502 Plus Chlorophyll Meter (Konica Minolta, Inc., Osaka, Japan). It determines the greenness of leaf and the interaction of incident light with thylakoid Chl (Jifon et al., 2005). Three SPAD readings per leaf (650/940 nm wavelength transmittance ratio) were taken at three points of each leaf, 15-35 mm from one side of the midrib (depending upon the leaf growth stage). Readings for 24 leaves per treatment (untreated, mock-inoculated, TYLCCNV A and TYLCCVN A + β infected *N. benthamiana* plants) were pooled to represent the relative Chl content in foliar tissues of untreated, mock-inoculated, and virus-infected *N. benthamiana* plants. Moreover, Arnon's method was used to prepare Chl extracts from wild type and *βC1* transgenic *N. benthamiana* plants (Arnon, 1949). Absorbance readings were recorded at 645 nm and 663 nm using a spectrophotometer. Calculation of photosynthetic pigments was performed using the equations described earlier (Arnon, 1949).

Chl fluorescence measurements. Measurement of Chl fluorescence parameters was done using a mini Pulse Amplitude Modulation (PAM-2000, Heinz Walz GmbH, Effeltrich, Germany) fluorometer without detaching the leaves. Following a dark adaptation period for 30 min, the background fluorescence signal (F_0) was measured with leaf tissue subjected to weak modulated measuring light (0.03 µmol/m^2/s). Then, a saturating pulse (8,000 µmol/m^2/s) was applied for 1 s to measure the maximum fluorescence emission (F_m). The F_m was further used to calculate F_v/F_m = $[(F_m - F_0)/F_m)]$ ratio. This ratio of F_v/F_m is called maximum

quantum yield of photosystem II (PSII) photochemistry, which has been widely used as an estimate of PSII photochemical efficiency as described earlier (Björkman and Demmig, 1987). In addition to F_v/F_m, other Chl fluorescence parameters including nonphotochemical quenching (*NPQ*), photochemical quenching (*qP*) coefficients and relative electron transport rate (ETR) were also measured (Baker, 2008; Bonfig et al., 2006; Rolfe and Scholes, 2010) in untreated, mock-inoculated, and virus-infected *N. benthamiana* plants. For each treatment, systemic and inoculated leaves were measured using the same saturation pulse intensity.

As the *βC1* transgenic *N. benthamiana* plants have deformed needle-like leaves that could not fit into PAM mini, the Chl fluorescence parameters of them were measured using full plants with a FluorCam 800MF Chl fluorescence imaging system (Photon System Instruments, Prague, Czech Republic). FluorCam 7.0 software was used to analyze and process the images from FluorCam 800MF. Following a dark adaptation of 30 min, plants were continuously kept in darkness during the period of fluorescence measurement. *QY-max* (equal to F_v/F_m), steady-state nonphotochemical quenching in light (*NPQ-Lss*) and steady-state fluorescence decline ratio in light (*Rfd-Lss*) were measured to evaluate the photosynthetic efficiency of the plants. False color was used to display the images. Measurements of 10 plants per treatment (wild type or *βC1* transgenic *N. benthamiana*) were combined to obtain average Chl fluorescence values. PRISM 5.01 (GraphPad Software, San Diego, CA, USA) was used for statistical analysis of the data.

RNA extraction, cDNA synthesis, and reverse transcription quantitative PCR (RT-qPCR). Total RNA was extracted from untreated, mock-inoculated, TYLCCNV A– and TYLCCNV A + β– infected *N. benthamiana* leaves at 5- and 14-day post-inoculation (dpi) using TRIZOL Reagent (Life Technologies, Inc., Gaithersburg, MD, USA) following manufacturer's instructions. The RNA quantity was assessed by A260/A280 ratio using NanoDrop 2000 Spectrophotometer (Thermo Fisher Scientific, Carlsbad, CA, USA). The integrity of RNA was analyzed by 0.8% agarose gel electrophoresis.

cDNA synthesis from total RNA was performed using the PrimeScript RT Master Mix reagent kit (Takara Biomedical Technology Co., Ltd., Beijing, China) following the manufacturer's instructions. The cDNA was stored at –80°C for downstream applications.

For RT-qPCR, a reaction mixture containing 1× SYBR Premix Ex Taq II, 0.4 μM forward and reverse primers, 2 μl of cDNA, and 8.5 μl of H_2O was prepared. Quantitative PCR was performed using a real-time PCR system (LightCycler 96, Roche, Basel, Switzerland). The glyceradehyde 3-phosphate dehydrogenase (*GAPDH*) was used as the reference gene to calculate the relative expression of target genes. All RT-qPCR reactions were performed using three biological and nine technical repeats, and the data were subjected to statistical analysis. The specific primer pairs for RT-qPCR were designed by using PrimerQuest program (Integrated DNA Technologies, Coralville, IW, USA). The primers' information is provided in Supplementary Table 1.

Nucleotide sequence accession numbers. GenBank accession numbers for the genes used in this study are as follows: *NbPsbO1* (JF897603), *NbPsbP1* (JF897607), *NbPsbQ1* (JF897611), and *NbPsbR* (Niben101Scf01116g01004.1).

Results

TYLCCNV A + β infection and transgene of βC1 induced abnormal phenotype in *N. benthamiana*. Without the presence of betasatellite, TYLCCNV A itself is a mild virus. TYLCCNV A infection triggered no obvious symptoms comparing to the untreated or mock-inoculated *N. benthamiana* plants. In TYLCCNV A + β co-infected plants, with the presence of DNAβ, visible disease symptoms appeared at 5-6 dpi. At this point, the leaves that were fully expanded at the time of inoculation did not produce any symptoms, whereas the systemic leaves (developed after inoculation) exhibited curling and wrinkling, but still remained green. However, as the infection progressed and the viral symptoms severed, the wrinkled curly leaves gradually turned yellow with obvious stunting of the plants (Fig. 1A and B). Similarly, transgenic plants expressing *35S::βC1* also produced deformed leaves with needle-like structure and were accompanied by stunted growth (Fig. 1C-F).

Relative Chl contents were decreased in TYLCCNV A-, TYLCCNV A + β–infected and βC1 transgenic *N. benthamiana*. Total Chl contents (Chl *a* + Chl *b*) of the untreated, mock-inoculated, TYLCCNV A– and TYLCCNV A + β–infected and *βC1* transgenic *N. benthamiana* plants were measured by SPAD. At 3-4 dpi, the relative chl contents in systemic and inoculated leaves of the virus-infected plants were similar to that of the control (untreated) plants. As the infection developed, the relative Chl contents of the infected plants started to decline in both systemic and inoculated leaves comparing to that of the controls. In the

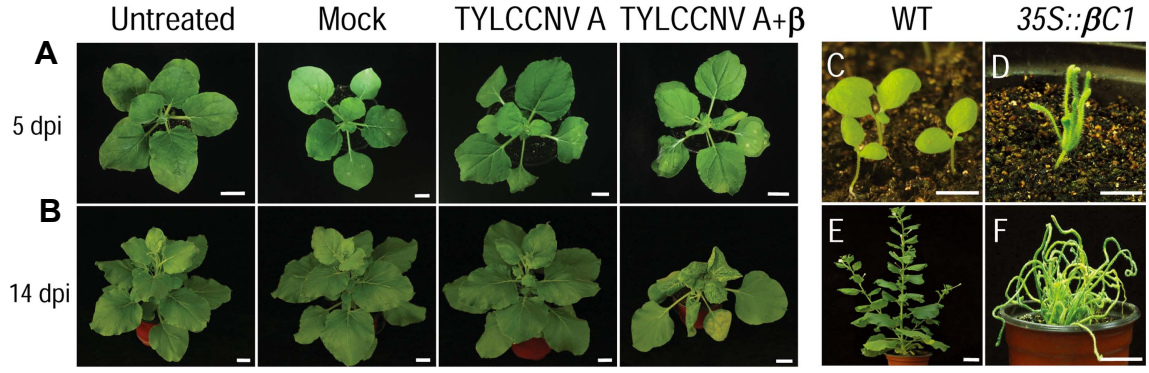

Fig. 1. Tomato yellow leaf curl China virus (TYLCCNV) infection and *βC1* transgene induce abnormal phenotype in *Nicotiana benthamiana*. (A, B) Images of the untreated, mock-inoculated, TYLCCNV A and TYLCCNV A + β co-infected *N. benthamiana* plants at 5-day post-inoculation (dpi) and 14 dpi, respectively. Scale bars = 3 cm. (C, D) Seedlings of the wild type (WT) and *35S::βC1*-transgenic *N. benthamiana* plants. Scale bars = 0.5 cm. (E, F) The WT and *35S::βC1* transgenic *N. benthamiana* plants at 2 months and 6 months after gemination respectively. Scale bars = 3 cm.

TYLCCNV A + β–infected plants, the decline of Chl content began early at 5-6 dpi. A similar decreasing trend was also observed in TYLCCNV A–infected plants. It started about 3 days later and was not as dramatic as that in the TYLCCNV A + β–infected ones. The decline in Chl contents continued and the divergence between TYLCCNV A– and TYLCCNV A + β–infected; between virus-infected and control plants became obvious with the progress of viral infection in both the systemic and inoculated leaves (Fig. 2A and B). Furthermore, the mock-inoculated plants exhibited Chl contents similar to that of the untreated *N. benthamiana* plants, indicating that buffer-only infiltration had no impact on Chl contents. At 14 dpi, the systemic leaves of mock- and TYLCCNV A–inoculated plants remained green, contrary to the yellowing of TYLCCNV A + β–inoculated plants (Fig. 1A and B). These results showed that TYLCCNV A alone triggered only a mild reduction in Chl content without obvious changes in the color of leaves, and the presence of DNAβ exacerbated the reduction. Also, the reduction of Chl content is independent of obvious viral symptoms. It happened before the onset of viral symptoms in TYLCCNV A + β–inoculated plants, and in TYLCCNV A–inoculated plants, which showed no obvious viral symptoms at all.

As the needle-like structure of the *βC1* transgenic *N. benthamiana* plants does not fit the leaf clip of SPAD, Arnon's method was applied to measure the Chl content of these tissues. The results showed that *βC1* transgenic plants contained significantly lower amounts of Chl *a*, Chl *b*, and total Chl comparing to the wild type (Fig. 2C). Taken together, both the TYLCCNV (A and A + *β*) infection and transgene of *βC1* resulted in a significant reduction in Chl contents, showing that *βC1* lowered Chl content and aggravated the chlorosis effect of TYLCCNV A during infection.

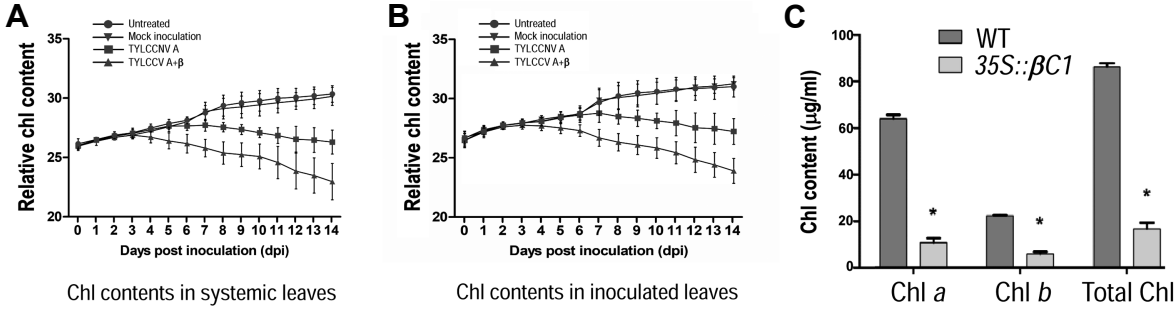

Fig. 2. βC1 reduces the chlorophyll contents in *Nicotiana benthamiana*. Estimation of the relative total chlorophyll (Chl) contents in systemic (A) and inoculated (B) leaves of untreated wild type (WT), mock-inoculated, Tomato yellow leaf curl China virus (TYLCCNV) A and TYLCCNV A + β–infected *N. benthamiana* plants. (C) The Chl concentration in the *βC1* transgenic and WT *N. benthamiana* calculated by Arnon's method. *Significant differences between the samples ($P < 0.05$). Error bar represents standard deviation ($n = 24$).

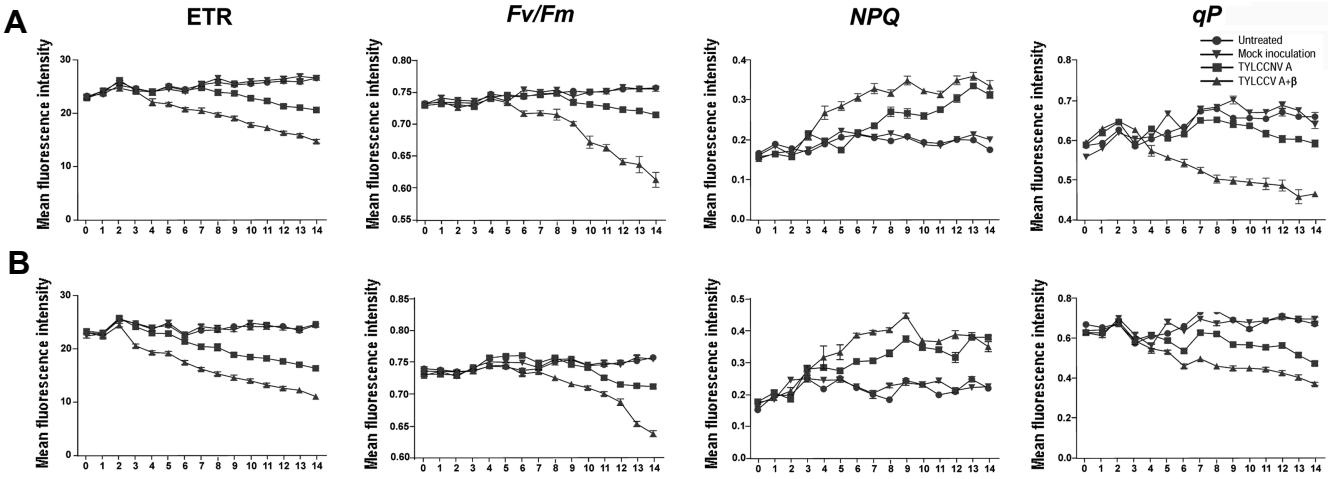

Fig. 3. Chlorophyll fluorescence parameters of the Tomato yellow leaf curl China virus (TYLCCNV)-infected *Nicotiana benthamiana* plants. Chlorophyll fluorescence parameters in systemic (A) and inoculated (B) leaves of the untreated, mock-inoculated, TYLCCNV A and TYLCCNV A + β–infected *N. benthamiana* plants at 0-14-day post-inoculation (dpi). Error bar represents standard deviation ($n = 9$). ETR, relative electron transport rate; *NPQ*, nonphotochemical quenching; *qP*, photochemical quenching.

Photosynthetic efficiency was hindered in TYLCCNV A–, TYLCCNV A+β–infected and βC1 transgenic *N. benthamiana*. Changes in Chl fluorescence parameters were measured to determine the photosynthetic efficiency in both systemic and inoculated leaves of the untreated, mock-inoculated, TYLCCNV A– and TYLCCNV A + β–infected *N. benthamiana* plants. Comparison was done for the Chl fluorescence parameters including ETR, F_v/F_m, *NPQ*, and *qP* in systemic (Fig. 3A) and inoculated leaves (Fig. 3B). These Chl fluorescence parameters were stable in both systemic and inoculated leaves of all the treatments till 3 dpi. After 3 dpi, the changes of fluorescence parameters in TYLCCNV A– and TYLCCNV A + β–infected plants reflected a decrease of photosynthetic efficiency. A progressive aggravation in photosynthetic efficiency was detected in the course of infection by TYLCCNV A and by TYLCCNV A + β, reflecting the accumulating viral damaging effect on the infected plants. For the plants infected with TYLCCNV A, changes of these photosynthesis parameters followed similar trends with those of the TYLCCNV A + β–infected ones, though initiated with a delay at around 7 dpi and developed less intensively. As for the mock-inoculated plants, they showed no variations in fluorescence parameters comparing to the untreated ones, indicating that the changes in plants' photosynthetic machinery were not caused by the inoculation process but by the viral infection.

Additionally, by using FluorCam, three Chl fluorescence parameters (*NPQ-Lss*, *Rfd-Lss*, and *QY-max*) were mea-

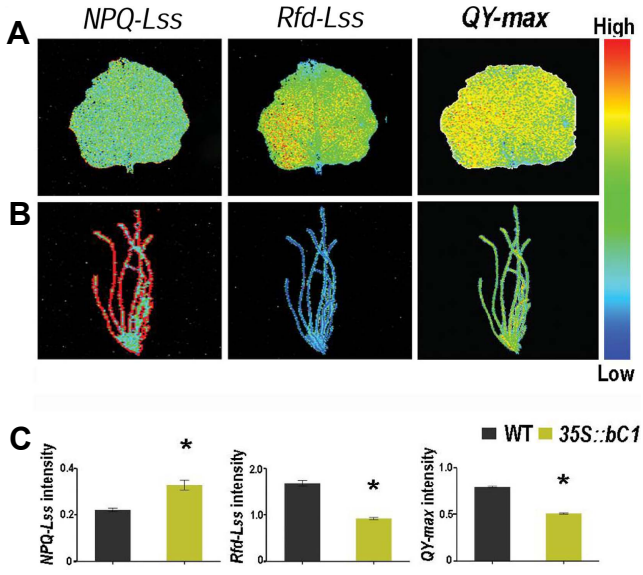

Fig. 4. Chlorophyll fluorescence images of the wild type and *βC1* transgenic *Nicotiana benthamiana* leaves. Chlorophyll fluorescence images of the *N. benthamiana* wild type (A) and *βC1* transgenic (B) leaves were measured under the same conditions. False color scale bar represents the signal intensity. The representative images for each treatment are shown. (C) Chlorophyll fluorescence parameters measured in the wild type and *βC1* transgenic plants. *NPQ-Lss*, nonphotochemical quenching in light; *Rfd-Lss*, steady-state fluorescence decline ratio in light. *Significant differences between chlorophyll fluorescence parameters of the *βC1* transgenic plants and the wild type ($P < 0.05$). Error bar represents standard deviation ($n = 10$).

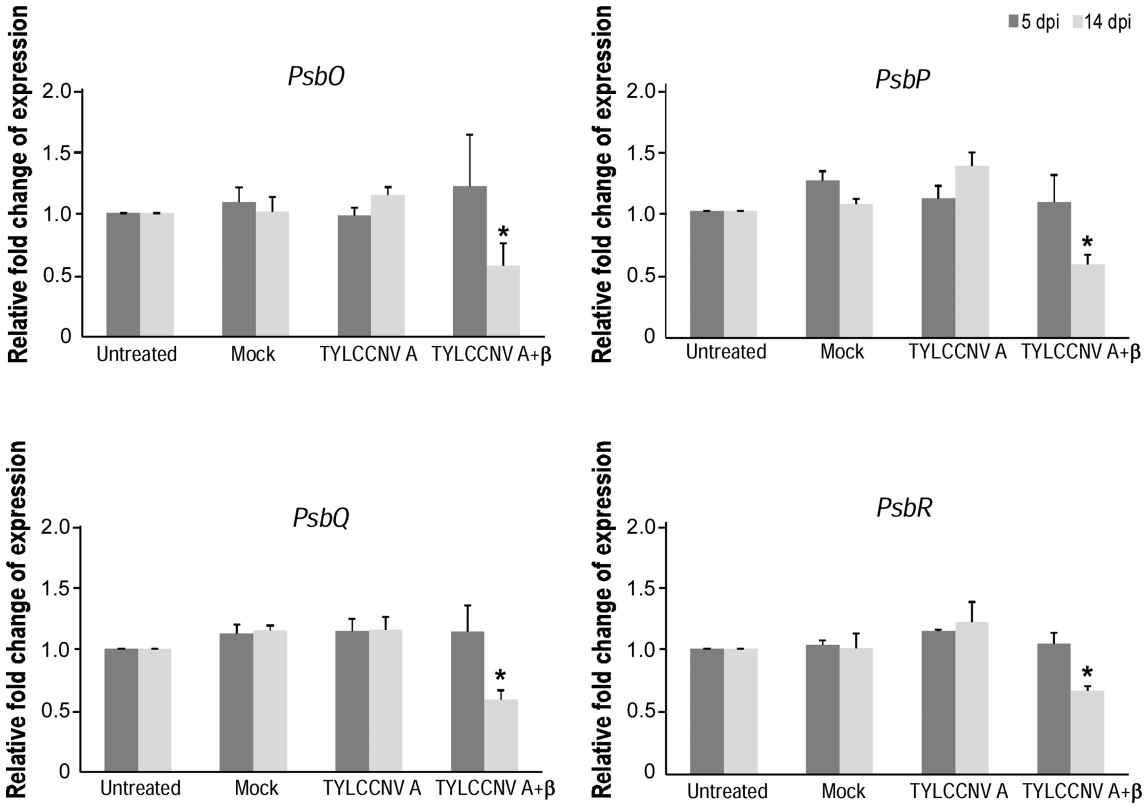

Fig. 5. Tomato yellow leaf curl China virus (TYLCCNV) infection reduced the relative expression of major photosystem II (PSII) extrinsic genes. Real-time quantitative PCR analysis was performed to determine the relative expression levels of the PSII genes, *PsbO*, *PsbP*, *PsbQ*, and *PsbR*, in untreated, mock-inoculated, TYLCCNV A and TYLCCNV A + β–infected *Nicotiana benthamiana* plants at 5- and 14-day post-inoculation (dpi). Relative expressions were normalized to those of the untreated plants, which were set to artificial values of 1. *Significant differences between transcription levels of *Psb* genes in the TYLCCNV A + β–infected plants at 5 and 14 dpi ($P < 0.05$). Error bar represents standard deviation ($n = 9$).

sured in the *35S::βC1* transgenic *N. benthamiana* plants with wild type as the controls. The fluorescence images of these parameters showed that the *βC1* transgenic *N. benthamiana* was reduced in photosynthesis efficiency (Fig. 4). The *NPQ-Lss* was much higher in the *βC1* transgenic plants than in wild type, while *Rfd-Lss*, which represents plant's vitality, and *QY-max*, which is equivalent to F_v'/F_m', were decreased in the *βC1* transgenic plants. Taken together, the changes in Chl fluorescence parameters reflected the decrease of photosynthetic potential in *βC1* transgenic plants, which suggested a negative impact of *βC1* on photosynthesis.

Expression of PSII-related genes was significantly reduced under prolonged influence of βC1. Inhibition of photosynthesis might be due to a reduction/alteration in expression of photosynthesis-related enzymes. PsbO, PsbP, PsbQ, and PsbR are four PSII extrinsic proteins that comprise the OEC of PSII (Sasi et al., 2018). Reduced PSII efficiency has been reported to be associated with changes in the expression of these major components of OEC (Bhattacharyya and Chakraborty, 2018; Pérez-Bueno et al., 2004; Sasi et al., 2018). To investigate the possible changes in transcription of these genes which might be induced by TYLCCNV infection or viral factor βC1, RT-qPCR analysis was performed for the 5 and 14 dpi samples. The transcript levels of OEC genes were analyzed in the systemic leaves of untreated, mock-inoculated, TYLCCNV A– and TYLCCNV A+β–infected *N. benthamiana* plants using *GAPDH* as an internal standard for relative quantification.

The results showed that the transcription levels of *PsbO*, *PsbP*, *PsbQ*, and *PsbR* remained unchanged at 5 dpi. However, a significant downregulation of these genes was observed in TYLCCNV A + β–infected plants at 14 dpi comparing to the untreated controls or plants with other treatments (Fig. 5). The reduced expression of these important PSII genes at 14 dpi in the TYLCCNV A + β–infected plants is consistent with the severe downregulation of

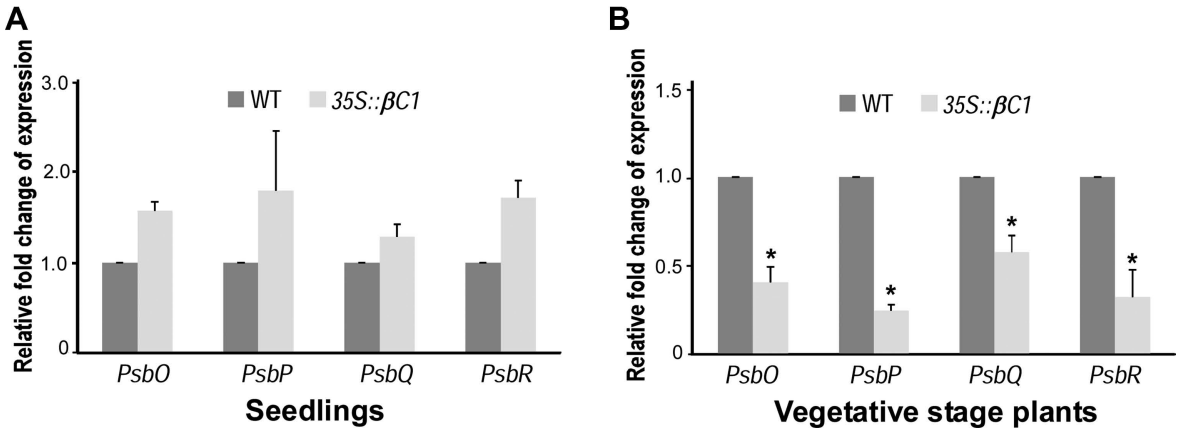

Fig. 6. *βC1* transgene reduced the expression of oxygen evolving complex (OEC) genes at vegetative stage. (A) Relative expression of OEC genes at the seedling stage. (B) Relative expression of OEC genes at the vegetative stage. Relative transcription levels of *PsbO*, *PsbP*, *PsbQ*, and *PsbR* were normalized to those of the wild-type (WT) plants, which were set to artificial values of 1. *Significant differences between transcription levels of *Psb* genes in the *βC1* transgenic plants and the WT ($P < 0.05$). Error bar represents standard deviation ($n = 9$).

photosynthesis efficiency judging from the photosynthetic parameters.

Furthermore, the expression of *PsbO*, *PsbP*, *PsbQ*, and *PsbR* was also measured in the *βC1* transgenic *N. benthamiana* plants at seedling stage and vegetative stage and compared with the expression of these genes in wild type at the same developmental stage. The transcription of these photosynthesis genes was significantly reduced in *βC1*-transgenic plants at the vegetative stage comparing to those of wild type at the vegetative stage (Fig. 6B). However, an upregulation of the expression of these genes was observed in the *βC1* transgenic *N. benthamiana* plants at the seedling stage (Fig. 6A). These results indicate that *βC1* reduces the transcription of OEC genes in the *βC1* transgenic *N. benthamiana* plants only after prolonged impact.

Discussion

In plant-virus interactions, chloroplast is a major target of viruses for their propagation or pathogenesis (Zhao et al., 2016). The virus-mediated disturbance of chloroplast structure and function not only leads to the development of disease symptoms but also results in reduced photosynthesis and changed expression of chloroplast/photosynthesis-related factors (Zhao et al., 2016). The monopartite begomoviruses are associated with alphasatellites/betasatellites which contribute to induction or enhancement of the disease symptoms. The geminiviruses betasatellite-encoded *βC1* gene acts as a symptom determinant, suppresses transcriptional or posttranscriptional gene silencing and affects jasmonic acid responsive genes (Zhou, 2013). βC1 of RaLCB has been reported to reduce the amount of Chl and alter the quantity of PSII-related proteins in *N. benthamiana* (Bhattacharyya et al., 2015). In this study, we determined the effect of TYLCCNV and its betasatellite-encoded pathogenicity factor, βC1, on the compromised photosynthetic capability in *N. benthamiana*.

Our study revealed that decrease of the Chl contents in TYLCCNV A–infected *N. benthamiana* started at 6-7 dpi, while in TYLCCNV A + β–infected *N. benthamiana*, the decrease of Chl started earlier at 3-4 dpi, displaying the aggravating effect of DNAβ on photosystem during TYLCCNV infection. As the mock-inoculated *N. benthamiana* exhibited no difference in Chl content comparing to the untreated controls, the photosynthesis-related changes solely came from viral infection. On the other hand, the amount of Chl *a* and Chl *b* in *βC1* transgenic *N. benthamiana* were lower than that of the wild type plants (Fig. 2), manifesting the detrimental effect of *βC1* in plant photosynthesis. Thus, our data are consistent with the previous findings in which *βC1* was associated with reduced Chl amounts and development of yellowing symptoms (Bhattacharyya et al., 2015; Funayama-Noguchi and Terashima, 2006; Rong et al., 2018).

Chl fluorescence imaging is a noninvasive technique in analyzing the dynamics of photosynthesis (Chaerle and Van der Straeten, 2000; Chaerle et al., 2004; Lei et al., 2016). Viral infection can induce chlorosis and Chl fluorescence changes in plants, reflecting the impaired photosynthetic complex and degraded chloroplasts (Lei et al., 2016). In this study, we used Chl fluorescence imaging to probe the PSII activities during TYLCCNV infection. Obvious

changes in fluorescence dynamics were observed in both TYLCCNV A– and TYLCCNV A + β–infected plants (Fig. 3). Remarkably, ETR, *NPQ*, and *qP* even displayed changes before the onset of obvious viral symptoms in TYLCCNV A + β–infected plants, and ETR, *NPQ*, F_v/F_m, and *qP* all developed obvious changes after prolonged infection of TYLCCNV A. Thus, these parameters can be important "disease signatures" in diagnosing early-stage TYLCCNV A + β–infection or mild TYLCCNV A infection without symptoms. For Potato virus Y infection, *NPQ* was reported to be the most useful fluorescence parameter for assessing the viral effect, but no changes showed up in *NPQ* before the appearance of viral symptoms (Spoustová et al., 2013). However, in Pepper mild mottle virus (PMMoV)–infected *N. benthamiana* plants, the changes in *NPQ* were detected in both symptomatic and asymptomatic leaves (Barón et al., 2016), and Tobacco mosaic virus infection triggered a presymptomatic rise in Chl fluorescence intensity in tobacco (Chaerle et al., 2004). In our research, we found that ETR, *NPQ*, F_v/F_m, and *qP* were affected in both symptomatic and asymptomatic leaves, during infection by both TYLCCNV A and TYLCCNV A + β, with the coinfection of DNAβ bringing more severe damages to plants' photosynthesis efficiency.

Impairment in photosynthesis has been documented in several reports on virus-infected plants (Barón et al., 2016; Bhattacharyya et al., 2015; Chaerle et al., 2004; Lohaus et al., 2000; Pérez-Bueno et al., 2006; Pineda et al., 2008, 2011; Spoustová et al., 2013; Zhao et al., 2016). PSII is a component of plants' photosynthetic machinery that is susceptible to environmental stresses (Nath et al., 2013). OEC subunits (*PsbO*, *PsbP*, *PsbQ*, and *PsbR*) play a critical role in oxygen evolution and any change in their expression drastically affects PSII efficiency (Sasi et al., 2018). OEC of PSII has been reported as a target of the tobamoviruses (Bhattacharyya and Chakraborty, 2018). PMMoV infection of *N. benthamiana* induces PSII inhibition by disturbing the OEC and results in decreased accumulation of PsbP and PsbO protein as the infection progresses (Pérez-Bueno et al., 2004). Our data disclosed that downregulation of the expression of *PsbO*, *PsbP*, *PsbQ*, and *PsbR* happened at the late stage of TYLCCNV A + β–infection, at 14 dpi, but not at the early stage of 5 dpi. In addition, TYLCCNV A–only infection triggered no expression changes of OEC genes (Fig. 5). These findings suggest that the OEC genes are not direct targets of TYLCCNV A. Moreover, in the plants with *βC1* transgene, the expression of OEC genes was significantly decreased in the vegetative stage plants but not in seedlings (Fig. 6B). Although we lack appropriate explanation for the upregulation of OEC genes in *βC1* transgenic seedlings (Fig. 6A), it is still deducible that *βC1* is not a direct target for downregulation of these OEC genes either.

Thus, our results demonstrate that TYLCCNV infection can induce reduction of Chl content and photosynthesis efficiency, with or without the effect of *βC1*. *βC1* is a damaging factor, the presence of which not only causes visible viral symptoms, but also aggravates the impairment of photosynthesis. The infection of TYLCCNV A did not induce significant changes in the expression of OEC genes. Whereas *βC1*, either in the form of betasatellite to be coinfected with TYLCCNV A or as overexpression of *βC1* in transgenic plants, was associated with downregulation of OEC genes after prolonged TYLCCNV A + β–infection and in *βC1* transgenic plants at late vegetative stage. Therefore, *βC1* probably influences photosynthesis rather than a direct effect on reducing the expression of OEC gene. Nonetheless, the downregulation of OEC genes can in turn impair the photosystem already harmed by viral infection, and *βC1* indeed contributes the impairment of photosynthesis as a pathogenicity factor.

Acknowledgments

This research was supported by the National Natural Science Foundation of China (31672006). We apologize for not being able to cover or cite all the achievements in photosynthesis-related viral research.

We thank technical editor, Carl Frederick Rupprecht (Marconi Communications, Inc., USA) for thoroughly reading and editing this manuscript in grammar and words.

Electronic Supplementary Material

Supplementary materials are available at The Plant Pathology Journal website (http://www.ppjonline.org/).

References

Arnon, D. I. 1949. Copper enzymes in isolated chloroplasts: polypenoloxidase in *Beta vulgaris*. *Plant Physiol.* 24:1-15.

Baker, N. R. 2008. Chlorophyll fluorescence: a probe of photosynthesis *in vivo*. *Annu. Rev. Plant Biol.* 59:89-113.

Barón, M., Pineda, M. and Pérez-Bueno, M. L. 2016. Picturing pathogen infection in plants. *Z. Naturforsch. C* 71:355-368.

Bhattacharyya, D. and Chakraborty, S. 2018. Chloroplast: the Trojan horse in plant-virus interaction. *Mol. Plant Pathol.* 19:504-518.

Bhattacharyya, D., Gnanasekaran, P., Kumar, R. K., Kushwaha, N. K., Sharma, V. K., Yusuf, M. A. and Chakraborty, S. 2015. A geminivirus betasatellite damages the structural and func-

tional integrity of chloroplasts leading to symptom formation and inhibition of photosynthesis. *J. Exp. Bot.* 66:5881-5895.

Björkman, O. and Demmig, B. 1987. Photon yield of O_2 evolution and chlorophyll fluorescence characteristics at 77 K among vascular plants of diverse origins. *Planta* 170:489-504.

Bonfig, K. B., Schreiber, U., Gabler, A., Roitsch, T. and Berger, S. 2006. Infection with virulent and avirulent *P. syringae* strains differentially affects photosynthesis and sink metabolism in *Arabidopsis* leaves. *Planta* 225:1-12.

Brown, J. K., Fauquet, C. M., Briddon, R. W., Zerbini, F. M., Moriones, E. and Navas-Castillo, J. 2012. Family *Geminiviridae*. In: *Virus Taxonomy: 9th Report of the International Committee on Taxonomy of Viruses*, eds. by A. King, E. Lefkowitz, M. J. Adams and E. B. Carstens, pp. 351-373. Elsevier, London, UK.

Chaerle, L., Hagenbeek, D., Bruyne, E. D., Valcke, R. and Van Der Straeten, D. 2004. Thermal and chlorophyll-fluorescence imaging distinguish plant-pathogen interactions at an early stage. *Plant Cell Physiol.* 45:887-896.

Chaerle, L. and Van der Straeten, D. 2000. Imaging techniques and the early detection of plant stress. *Trends Plant Sci.* 5:495-501.

Cui, X., Tao, X., Xie, Y., Fauquet, C. M. and Zhou, X. 2004. A DNAβ associated with *Tomato yellow leaf curl China virus* is required for symptom induction. *J. Virol.* 78:13966-13974.

Funayama-Noguchi, S. and Terashima, I. 2006. Effects of *Eupatorium* yellow vein virus infection on photosynthetic rate, chlorophyll content and chloroplast structure in leaves of *Eupatorium makinoi* during leaf development. *Funct. Plant Biol.* 33:165-175.

Inoue-Nagata, A. K., Lima, M. F. and Gilbertson, R. L. 2016. A review of geminivirus diseases in vegetables and other crops in Brazil: current status and approaches for management. *Hortic. Bras.* 34:8-18.

Jifon, J. L., Syvertsen, J. P. and Whaley, E. 2005. Growth environment and leaf anatomy affect nondestructive estimates of chlorophyll and nitrogen in *Citrus* sp. leaves. *J. Am. Soc. Hortic. Sci.* 130:152-158.

Lei, R., Jiang, H., Hu, F., Yan, J. and Zhu, S. 2016. Chlorophyll fluorescence lifetime imaging provides new insight into the chlorosis induced by plant virus infection. *Plant Cell Rep.* 36:327-341.

Leke, W. N., Mignouna, D. B., Brown, J. K. and Kvarnheden, A. 2015. Begomovirus disease complex: emerging threat to vegetable production systems of West and Central Africa. *Agric. Food Secur.* 4:1.

Lohaus, G., Heldt, H. W. and Osmond, C. B. 2000. Infection with phloem limited *Abutilon* mosaic virus causes localized carbohydrate accumulation in leaves of *Abutilon striatum*: relationships to symptom development and effects on chlorophyll fluorescence quenching during photosynthetic induction. *Plant Biol.* 2:161-167.

Nath, K., Jajoo, A., Poudyal, R. S., Timilsina, R., Park, Y. S., Aro, E.-M., Nam, H. G. and Lee, C.-H. 2013. Towards a critical understanding of the photosystem II repair mechanism and its regulation during stress conditions. *FEBS Lett.* 587:3372-3381.

Pérez-Bueno, M. L., Ciscato, M., VandeVen, M., García-Luque, I., Valcke, R. and Barón, M. 2006. Imaging viral infection: studies on *Nicotiana benthamiana* plants infected with the pepper mild mottle tobamovirus. *Photosynth. Res.* 90:111-123.

Pérez-Bueno, M. L., Rahoutei, J., Sajnani, C., García-Luque, I. and Barón, M. 2004. Proteomic analysis of the oxygen-evolving complex of photosystem II under biotec stress: studies on *Nicotiana benthamiana* infected with tobamoviruses. *Proteomics* 4:418-425.

Pineda, M., Olejníčková, J., Cséfalvay, L. and Barón, M. 2011. Tracking viral movement in plants by means of chlorophyll fluorescence imaging. *J. Plant Physiol.* 168:2035-2040.

Pineda, M., Soukupová, J., Matouš, K., Nedbal, L. and Baron, M. 2008. Conventional and combinatorial chlorophyll fluorescence imaging of tobamovirus-infected plants. *Photosynthetica* 46:441-451.

Rolfe, S. A. and Scholes, J. D. 2010. Chlorophyll fluorescence imaging of plant–pathogen interactions. *Protoplasma* 247:163-175.

Rong, W., Wang, X., Wang, X., Massart, S. and Zhang, Z. 2018. Molecular and ultrastructural mechanisms underlying yellow dwarf symptom formation in wheat after infection of barley yellow dwarf virus. *Int. J. Mol. Sci.* 19:1187.

Sasi, S., Venkatesh, J., Daneshi, R. F. and Gururani, M. A. 2018. Photosystem II extrinsic proteins and their putative role in abiotic stress tolerance in higher plants. *Plants* 7:100.

Spoustová, P., Synková, H., Valcke, R. and Čeřovská, N. 2013. Chlorophyll *a* fluorescence as a tool for a study of the *Potato virus Y* effects on photosynthesis of nontransgenic and transgenic P*ssu-ipt* tobacco. *Photosynthetica* 51:191-201.

Zhang, J., Dang, M., Huang, Q. and Qian, Y. 2015. Determinants of disease phenotype differences caused by closely-related isolates of begomovirus betasatellites inoculated with the same species of helper virus. *Viruses* 7:4945-4959.

Zhao, J.. Zhang, X., Hong, Y. and Liu, Y. 2016. Chloroplast in plant-virus interaction. *Front. Microbiol.* 7:1565.

Zhou, X. 2013. Advances in understanding begomovirus satellites. *Annu. Rev. Phytopathol.* 51:357-381.